

To be submitted to  
Physics Letters B

COMITATO NAZIONALE PER L'ENERGIA NUCLEARE  
Laboratori Nazionali di Frascati

LNF-76/17(P)  
11 Marzo 1976

R. Dymarz and A. Małecki : A NEW METHOD FOR SOLVING  
THE SCHROEDINGER EQUATION OF SCATTERING. -

LNF-76/17(P)  
11 Marzo 1976

R. Dymarz<sup>(x)</sup> and A. Małecki : A NEW METHOD FOR SOLVING THE SCHROEDINGER EQUATION OF SCATTERING. -

ABSTRACT.-

We present a method of calculating the scattering phase-shifts for an optical-model potential. The method which consists in approximating the potential by a sum of rectangular wells, turns out to be very useful, especially at large values of the c. m. momentum.

The optical model of nuclear collisions encounters serious difficulties in calculating the scattering amplitudes at large values of the centre-of-mass momentum  $k$ . The large wave-numbers  $k$  ( $\gtrsim 5 \text{ fm}^{-1}$ ) occur at high energies in nucleon-nucleus scattering, and at moderate energies for collisions of two nuclei. The difficulties are the greatest at large scattering angles where the cross-sections are very small.

The large value of  $k$  necessitates the inclusion of many terms in the partial-wave expansion of the elastic scattering amplitude :

$$F(\theta) = F_c + \frac{i}{2k} \sum_{l=0}^{\infty} (2l+1) e^{2i\sigma_l} (1 - e^{2i\delta_l}) P_l(\cos \theta), \quad (1)$$

$F_c$  being the scattering amplitude for the point Coulomb potential,  $\sigma_l$  the Coulomb phase-shifts, and  $P_l$  the Legendre polynomials.

At large angles  $\theta$  the individual terms in (1) have to be calculated very accurately since the small cross-sections result from a great

---

(x) - From Institute of Nuclear Physics, Cracow (Poland).

2.

amount of cancellations in the partial-wave sum. The essential problem is a precise calculation of the scattering phase-shifts  $\delta_1$ . They are obtained by matching at a large radius  $r = R_M$  the radial wave functions  $R_1(r)$ , corresponding to a given optical-model potential, with a linear combination of regular  $F_1(kr)$  and irregular  $G_1(kr)$  Coulomb wave functions<sup>(1)</sup>:

$$e^{2i\delta_1} \equiv S_1 = - \frac{kC_1^{(-)}(kR_M) - C_1^{(-)}(kR_M) \cdot H_1(R_M)}{kC_1^{(+)}(kR_M) - C_1^{(+)}(kR_M) \cdot H_1(R_M)}, \quad (2)$$

$$H_1 \equiv \frac{d}{dr} \ln R_1(r), \quad C_1^{(\pm)}(z) \equiv \frac{1}{z} [F_1(z) \mp iG_1(z)].$$

In standard optical-model codes the wave functions  $R_1$  are generated by numerically integrating the radial Schrödinger equation from the origin to  $R_M$ . This is accomplished with the aid of the Runge-Kutta or Fox-Goodwin<sup>(2)</sup> methods; the starting values being obtained approximating the solution by a few first terms in a Taylor series. The procedures require, at large wave-numbers  $k$ , a very small step of integration since the radial wave functions oscillate then many times over the extent of the nuclear potential.

The fact that the radial dependence of the potential is much smoother than that of the wave functions has motivated us to develop another method for calculating the phase-shifts. It consists in approximating the potential by a sum of rectangular wells (see Fig. 1):

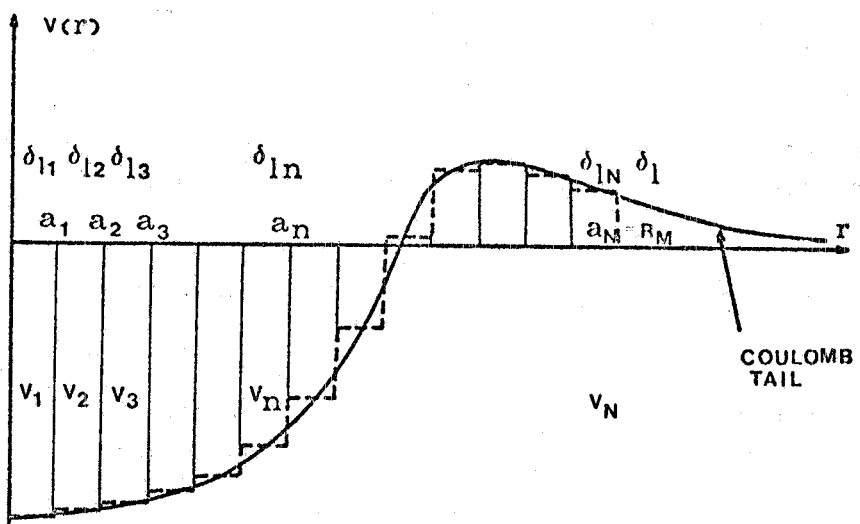


FIG. 1 - The exact (solid line) and the approximating (broken line) potential.

$$V(r) \approx \sum_{n=1}^N V_n, \quad \text{where} \quad (3)$$

$$V_n = \frac{1}{2} [V(a_{n-1}) + V(a_n)] \quad \text{for } a_{n-1} < r \leq a_n = n \frac{R_M}{N},$$

In contrast to the standard methods we will make use of the wave functions which are the exact solutions to the approximating potential, rather than approximate solutions to the exact potential. In fact, the radial wave functions, corresponding to the potential (3), can be calculated exactly:

$$R_I(r) = \sum_{n=1}^N R_{ln}(r), \quad \text{where} \quad (4)$$

$$R_{ln}(r) \sim e^{2i\delta_{ln}} h_1^{(+)}(K_n r) + h_1^{(-)}(K_n r) \quad \text{for } a_{n-1} < r \leq a_n,$$

$h_1^{(\pm)}(z)$  being the spherical Hankel functions (spherical Bessel functions of the third kind<sup>(1)</sup>).

The local wave-number  $K_n$  (generally complex) is :

$$K_n = (k^2 - 2EV_n)^{1/2} \quad \text{for } a_{n-1} < r \leq a_n, \quad (5)$$

E being the reduced energy (nonrelativistically - the reduced mass) of the two colliding nuclei.

From the conditions of continuity at the boundaries of the rectangular wells one obtains :

$$S_{ln} \equiv e^{2i\delta_{ln}} = - \frac{K_n h_1^{(-)}(K_n a_{n-1}) - h_1^{(-)}(K_n a_n) \cdot H_{ln}}{K_n h_1^{(+)}(K_n a_{n-1}) - h_1^{(+)}(K_n a_n) \cdot H_{ln}}, \quad (6)$$

where

$$H_{ln} = K_{n-1} \frac{S_{ln-1} h_1^{(+)}(K_{n-1} a_{n-1}) + h_1^{(-)}(K_{n-1} a_{n-1})}{S_{ln-1} h_1^{(+)}(K_{n-1} a_{n-1}) + h_1^{(-)}(K_{n-1} a_{n-1})}.$$

The recurrence relations (6), supplemented by the obvious condition  $S_{11} = 1$ , allow to compute  $H_1 = H_{LN+1}$  in Eq. (2), and hence the

4.

scattering matrix elements  $S_1$ . As for the Coulomb and Hankel functions there are precise procedures for calculating them<sup>(3, 4)</sup>.

Our method has been compared with the optical-model code JIB3<sup>(5)</sup>. To this end JIB3 has been modified by us so that the matching radius  $R_M$  and the maximum value of  $l = l_{\max}$  may be specified externally. Moreover, both in JIB3 and our program (called here SQUAR) we have applied the Coulomb procedure of Ref. (3).

The comparison has been made on the example of  $^{60}\text{Ni}(^3\text{He}, ^3\text{He})^{60}\text{Ni}$  scattering at 71 MeV ( $k = 3.05 \text{ fm}^{-1}$ ), using the potential with an absorptive part peaked at the surface:

$$V(r) = -V_R f(x_R) + i4W_D \frac{d}{dx_I} f(x_I) + V_C , \quad \text{where} \\ f(x) = (1+e^x)^{-1}, \quad x_R = \frac{r - r_R A^{1/3}}{a_R} , \quad x_I = \frac{r - r_I A^{1/3}}{a_I} , \quad (7)$$

$V_C$  being the Coulomb potential corresponding to the point projectile charge on a uniformly charged sphere of radius  $R_c = r_c \cdot A^{1/3}$ . The parameters are  $V_R = 126.5 \text{ MeV}$ ,  $r_R = 1.12 \text{ fm}$ ,  $a_R = 0.837 \text{ fm}$ ,  $W_D = 20.4 \text{ MeV}$ ,  $r_I = 1.26 \text{ fm}$ ,  $a_I = 0.841 \text{ fm}$ , and  $r_c = 1.3 \text{ fm}$ . This case has been carefully studied in Ref. (6) with the aid of various optical-model codes.

In Table I the backward scattering differential cross-sections, resulting from JIB3 and SQUAR, are compared for various numbers of steps  $N$ . The other numerical accuracy parameters has been fixed as  $R_M = 25 \text{ fm}$ ,  $l_{\max} = 100$ . It may be observed that JIB3 fails at small number of division points. Instead the code SQUAR already at  $N = 200$  yields the cross-sections which are in only 10% error with respect to the exact results ( $N = 2000$ ). The faster convergence results from the fact that in our method we approximate the potential, rather than the wave functions.

This advantage of our method is particularly visible at larger values of the c.m. momentum  $k$ , as it illustrated in Table II. Here we have calculated the differential cross-sections for the  $^3\text{He}-^{60}\text{Ni}$  elastic scattering at  $k = 11.4$  and  $25.6 \text{ fm}^{-1}$ , using the same potential (7) and the parameters  $R_M$  and  $l_{\max}$ , as in the example at  $k = 3.05 \text{ fm}^{-1}$ . Of course, the restriction to  $l \leq 100$  is no longer valid at higher energies. Nevertheless, the results of Table II, although should not be taken to represent the actual cross-sections, may serve as a device for a comparison of the two methods. While for JIB3 the minimum number of steps  $N_{\min}$  required for an accurate result is rapidly increasing with  $k$ , in

**TABLE I** - The comparison of our method and the optical-model code JIB3 for the  ${}^3\text{He}-{}^{60}\text{Ni}$  elastic scattering at  $k = 3.05 \text{ fm}^{-1}$ .

Scattering angle (c.m.) $\theta$	Number of steps N	Differential cross-section (mb/sr) for ${}^{60}\text{Ni}({}^3\text{He}, {}^3\text{He}){}^{60}\text{Ni}$ at $k = 3.05 \text{ fm}^{-1}$	
		JIB3	SQUAR
$160^\circ$	100	$4.341 \times 10^{-5}$	$4.079 \times 10^{-6}$
	200	$6.383 \times 10^{-6}$	$4.259 \times 10^{-6}$
	400	$4.644 \times 10^{-6}$	$4.400 \times 10^{-6}$
	800	$4.477 \times 10^{-6}$	$4.441 \times 10^{-6}$
	2000	$4.466 \times 10^{-6}$	$4.454 \times 10^{-6}$
$170^\circ$	100	$8.211 \times 10^{-5}$	$1.282 \times 10^{-6}$
	200	$1.647 \times 10^{-6}$	$1.940 \times 10^{-6}$
	400	$2.167 \times 10^{-6}$	$2.158 \times 10^{-6}$
	800	$2.233 \times 10^{-6}$	$2.218 \times 10^{-6}$
	2000	$2.238 \times 10^{-6}$	$2.232 \times 10^{-6}$
$180^\circ$	100	$3.753 \times 10^{-6}$	$2.868 \times 10^{-5}$
	200	$2.973 \times 10^{-5}$	$2.643 \times 10^{-5}$
	400	$2.626 \times 10^{-5}$	$2.601 \times 10^{-5}$
	800	$2.594 \times 10^{-5}$	$2.596 \times 10^{-5}$
	2000	$2.592 \times 10^{-5}$	$2.591 \times 10^{-5}$

**TABLE II** - The comparison of our method and the optical-model code JIB3 for the  ${}^3\text{He}-{}^{60}\text{Ni}$  elastic scattering at  $k = 11.44 \text{ fm}^{-1}$  and  $k = 25.57 \text{ fm}^{-1}$ .

Scattering angle (c.m.) $\theta$	Number of steps N	Differential cross-section (mb/sr) for ${}^{60}\text{Ni}({}^3\text{He}, {}^3\text{He}){}^{60}\text{Ni}$			
		$k = 11.44 \text{ fm}^{-1}$		$k = 25.57 \text{ fm}^{-1}$	
		JIB3	SQUAR	JIB3	SQUAR
$86^\circ$	250	$1.463 \times 10^{-5}$	$5.515 \times 10^{-6}$	$4.999 \times 10^{-1}$	$7.860 \times 10^{-5}$
	500	$2.971 \times 10^{-6}$	$5.501 \times 10^{-6}$	$6.990 \times 10^{-4}$	$7.848 \times 10^{-5}$
	1000	$5.297 \times 10^{-6}$	$5.500 \times 10^{-6}$	$1.311 \times 10^{-4}$	$7.844 \times 10^{-5}$
	2000	$5.467 \times 10^{-6}$	$5.500 \times 10^{-6}$	$8.243 \times 10^{-5}$	$7.844 \times 10^{-5}$
	3000	$5.464 \times 10^{-6}$	$5.500 \times 10^{-6}$	$8.031 \times 10^{-5}$	$7.844 \times 10^{-5}$
$102^\circ$	250	$2.724 \times 10^{-3}$	$2.338 \times 10^{-5}$	$7.008 \times 10^{-1}$	$1.502 \times 10^{-3}$
	500	$4.385 \times 10^{-5}$	$2.326 \times 10^{-5}$	$2.023 \times 10^{-4}$	$1.502 \times 10^{-3}$
	1000	$2.401 \times 10^{-5}$	$2.322 \times 10^{-5}$	$1.842 \times 10^{-3}$	$1.502 \times 10^{-3}$
	2000	$2.320 \times 10^{-5}$	$2.322 \times 10^{-5}$	$1.518 \times 10^{-3}$	$1.502 \times 10^{-3}$
	3000	$2.319 \times 10^{-5}$	$2.322 \times 10^{-5}$	$1.500 \times 10^{-3}$	$1.502 \times 10^{-3}$
$168^\circ$	250	$2.200 \times 10^{-2}$	$2.104 \times 10^{-5}$	$2.041 \times 10^{+3}$	$4.456 \times 10^{-3}$
	500	$6.083 \times 10^{-5}$	$2.102 \times 10^{-5}$	$9.933 \times 10^{-2}$	$4.456 \times 10^{-3}$
	1000	$2.393 \times 10^{-5}$	$2.102 \times 10^{-5}$	$5.558 \times 10^{-3}$	$4.456 \times 10^{-3}$
	2000	$2.134 \times 10^{-5}$	$2.102 \times 10^{-5}$	$4.597 \times 10^{-3}$	$4.456 \times 10^{-3}$
	3000	$2.124 \times 10^{-5}$	$2.102 \times 10^{-5}$	$4.507 \times 10^{-3}$	$4.456 \times 10^{-3}$

6.

our method it is almost energy independent. From Table II it would even seem that our  $N_{\min}$  decreases with energy but it should also be kept in mind that  $N_{\min}$  depends on the magnitude of the actual cross-sections which will be different (smaller) from the numbers quoted in the Table.

In conclusion, the comparisons presented in Tables I and II demonstrate the utility of our method which gives, especially at large values of wave-number  $k$ , a considerable reduction of computing time.

The authors would like to thank Prof. P. Picchi for his continuous interest and discussions. The hospitality of Prof. G. Bellettini at the Laboratori Nazionali di Frascati is gratefully acknowledged.

REFERENCES. -

- (1) - M. Abramowitz and I. A. Stegun, Handbook of Mathematical Functions (National Bureau of Standards, Washington, 1965).
- (2) - L. Fox and E. T. Goodwin, Proc. Cambridge Phil. Soc. 45, 373 (1949).
- (3) - A. R. Barnet et al., Comput. Phys. Communic. 8, 377 (1974).
- (4) - CERN, Program Library, C 303.
- (5) - F. G. Perey, The optical model code JIB3 (unpublished).
- (6) - R. R. Doering, A. I. Galonsky and R. A. Hinrichs, Jnl. Comput. Physics 12, 498 (1973).